

PERSPECTIVE • OPEN ACCESS

## Future prospects for the design of ‘state-of-the-art’ solid oxide fuel cells

To cite this article: Toshiyuki Mori *et al* 2020 *J. Phys. Energy* **2** 031001

View the [article online](#) for updates and enhancements.

### You may also like

- [Electron probe microanalysis using oxygen x-rays: II. Absorption correction models](#)  
G Love, M G C Cox and V D Scott
- [The role of dopant segregation on the oxygen vacancy distribution and oxygen diffusion in CeO<sub>2</sub> grain boundaries](#)  
Adam R Symington, Marco Molinari, Joel Statham et al.
- [Microstructural and compositional optimization of La<sub>0.5</sub>Ba<sub>0.5</sub>CoO<sub>3</sub>—BaZr<sub>1-z</sub>Y<sub>z</sub>O<sub>3</sub> \(z = 0, 0.05 and 0.1\) nanocomposite cathodes for protonic ceramic fuel cells](#)  
Laura Rioja-Monllor, Carlos Bernuy-Lopez, Marie-Laure Fontaine et al.



## PERSPECTIVE

## OPEN ACCESS

## RECEIVED

26 December 2019

## REVISED

10 April 2020

## ACCEPTED FOR PUBLICATION

30 April 2020

## PUBLISHED

3 July 2020

Original content from this work may be used under the terms of the [Creative Commons Attribution 4.0 licence](#).

Any further distribution of this work must maintain attribution to the author(s) and the title of the work, journal citation and DOI.



## Future prospects for the design of ‘state-of-the-art’ solid oxide fuel cells

Toshiyuki Mori<sup>1</sup> , Roger Wepf<sup>2</sup> and San Ping Jiang<sup>3</sup>

<sup>1</sup> Center for Green Research on Energy and Environmental Materials, National Institute for Materials Science (NIMS), 1-1 Namiki, Tsukuba, Ibaraki 305-0044, Japan

<sup>2</sup> Centre for Microscopy and Microanalysis, The University of Queensland, St Lucia, Brisbane, Qld 4072, Australia

<sup>3</sup> WA School of Mines: Minerals, Energy and Chemical Engineering & Fuels and Energy Technology Institute, Curtin University, Kent Street, Bentley, Perth, WA, Australia

E-mail: [MORI.Toshiyuki@nims.go.jp](mailto:MORI.Toshiyuki@nims.go.jp) and [S.Jiang@curtin.edu.au](mailto:S.Jiang@curtin.edu.au)

**Keywords:** solid oxide fuel cells, multidisciplinary research team work, fusion of fabrication and modelling, interface microanalysis, state-of-the-art IT-SOFC

Solid oxide fuel cells (SOFCs) are the clean and efficient power sources for generating electricity from a variety of fuels (i.e. hydrogen, natural gas, and biogas) [1–3]. Also, SOFCs have no corrosive components and do not require precious-metal electrocatalysts due to the high operation temperatures (800 °C–1000 °C) [3]. In the recent research, the major target focuses on design of functional interfaces in SOFCs device and system for lowering the operation temperature of SOFCs to intermediate temperatures (IT-SOFCs, 400 °C–700 °C) in order to increase the operation durability, improve the thermal compatibility, and thermal cycle capability and reduce the fabrication and materials costs by using metallic interconnectors in the SOFC stack cell. In this endeavor, it is well-known that two major strategies have been adopted to increase the performance of single cells in the intermediate temperature region. One strategic challenge is the fabrication of thin electrolyte (thickness: less than 10 μm) with high density to minimize the ohmic loss of the electrolyte. And another one is the reduction of excess overpotentials observed for the O<sub>2</sub> reduction reaction at the cathode in the single cells [4].

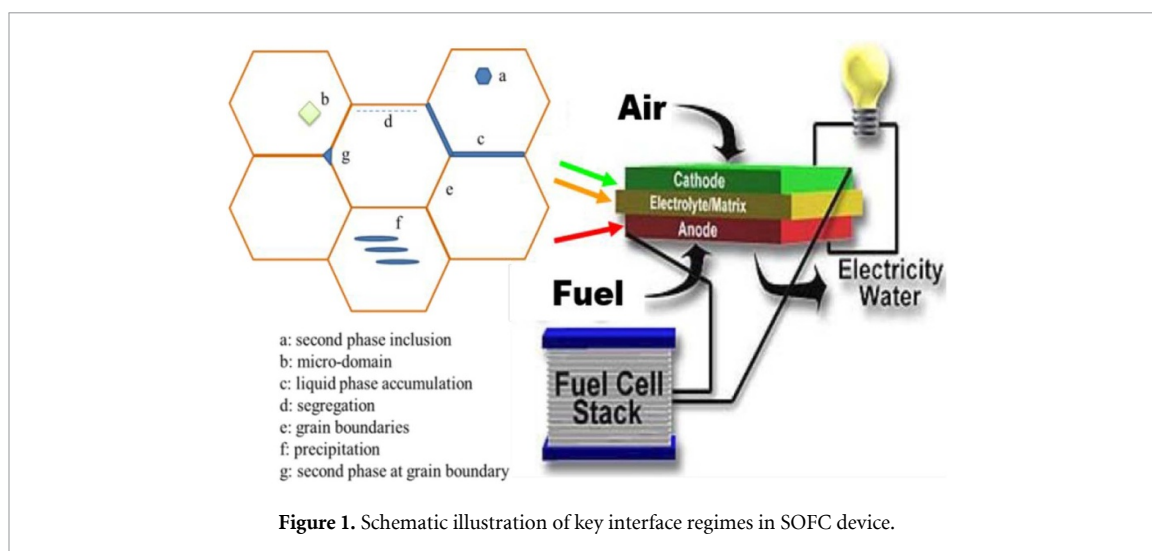
However, to develop the ‘state-of-the-art IT-SOFCs’ with quality of exceeding the limit of conventional IT-SOFCs, an advanced strategy for the design of key interfaces in SOFC devices and systems is required.

SOFC device and system contain a number of interface regimes which play key roles in the performance of SOFC device and system. The gas-solid interfaces on both cathode and anode assemblies control the charge transfer phenomena in the fuel cell reaction. Also, the three-phase boundary (TPB) at the electrode-electrolyte interface is a key active site area where both the electron exchange and formation of conduction ions take place. As a consequence of this, the key microstructure at the interface in SOFC devices has been discussed previously in the published literature [5].

A schematic representation of key interface regimes is illustrated in figure 1 [5]. The key interfaces of SOFC devices include (a) the second phase inclusion, (b) possible formation of ordered micro-domains, (c) liquid phase accumulation induced by impurity, (d) segregation effect, (f) precipitation in the matrix, or (g) second phase at grain boundary, as demonstrated in figure 1. In each case, the control of the interface structures at cathode/electrolyte, in the electrolyte and in the cermet anode layer can influence the performance of the IT-SOFC device. Therefore, we would like to summarize key points for development of IT-SOFCs in following sections.

## 1. Cathode and cathode/electrolyte interface

For the development of IT-SOFC devices, the first key endeavor is the design of the interface between cathode and electrolyte. Among the various kinds of previously proposed electrolyte, lanthanum strontium manganite (LSM) perovskite-based material is the most important cathode material in a SOFC device. It is because the LSM has an excellent track record of microstructural stability and long-term performance stability. However, the polarization performance and electrochemical activity of LSM based cathodes are a complex function of composition, the microstructure of cathode/electrolyte interface and activation effect. The key points for usage of LSM cathode in SOFC devices are summarized in the previously published review

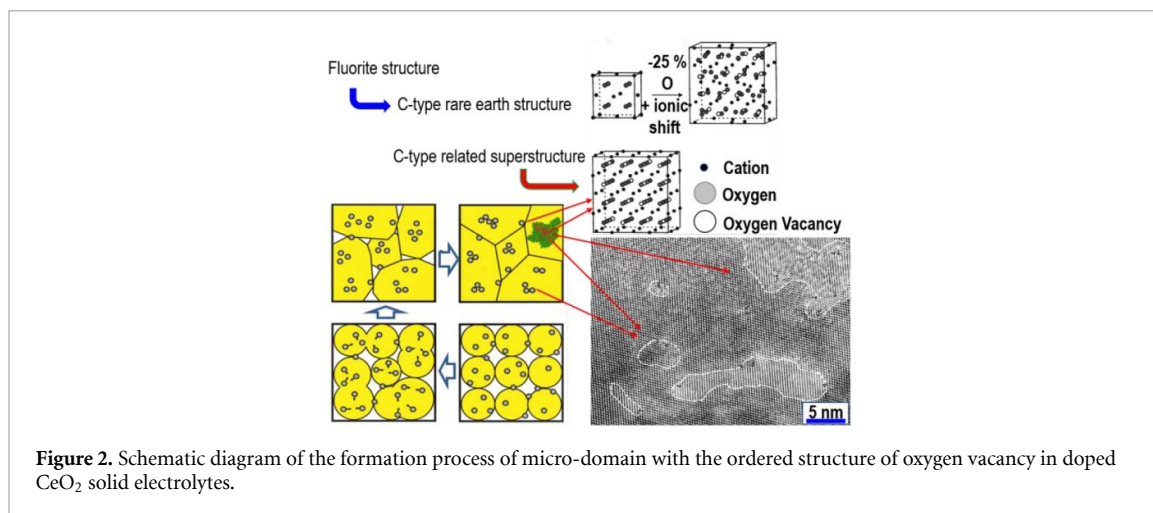


paper [6]. Usually, the LSM-based cathode is used for high-temperature SOFC devices, the electrocatalytic activity of LSM-based cathode can be substantially enhanced by the design of microstructure in nano-scale (e.g. by infiltration and impregnation of catalytic active and ‘mixed ionic and electronic conducting or MIEC’ nanoparticles) [7]. The performance of nanostructured LSM-based cathode is comparable to that of typical MIEC cathodes such as cobaltite-based perovskite cathodes (e.g.  $\text{Ba}_{0.5}\text{Sr}_{0.5}\text{Co}_{0.8}\text{Fe}_{0.2}\text{O}_{3-\delta}$  (BSCF),  $\text{La}_{0.6}\text{Sr}_{0.4}\text{Co}_{0.2}\text{Fe}_{0.8}\text{O}_{3-\delta}$  (LSCF) and  $\text{PrBa}_{0.5}\text{Sr}_{0.5}\text{Co}_{1.5}\text{Fe}_{0.5}\text{O}_{3-\delta}$  (PBSCF)). Among cobaltite-based perovskite cathodes, LSCF-based cathode is the most popular and representative MIEC cathode material for the development of IT-SOFC devices [8]. However, it was reported that the performance of IT-SOFC with LSCF cathode deteriorated by the surface segregation of Sr species and formation of Sr-rich reaction layer at the interface of the cathode/electrolyte of the single cell [9]. The previously published data suggests that the functional interfacial layer can be formed using MIEC highly ionic conducting nano-particles such as  $\text{Er}_{0.4}\text{Bi}_{1.6}\text{O}_3$  (ESB) decorated LSCF-based MIEC cathodes on barrier-layer-free YSZ electrolyte under SOFC operation condition [10]. The polarization induced ESB-rich interface is highly active for the  $\text{O}_2$  reduction reaction and inhibits the interfacial reaction between LSCF and YSZ by suppressing the Sr surface segregation.

In addition, a kinetics investigation of the oxygen reduction reaction on LSCF- $\text{Gd}_2\text{O}_3$  doped  $\text{CeO}_2$  (GDC) composite cathode suggested the origin of distortions in measured impedance spectrum arc observed for LSCF-GDC cathode [11]. Also, the model analysis of the reactive pathway at TPB on the basis of kinetics and thermodynamics is useful to understand the role of functional interface of LSCF- $\text{Gd}_2\text{O}_3$  doped  $\text{CeO}_2$  composite cathode [12]. The conventional modelling on the basis of ideal interface structure of MIEC cathode would be useful to optimize the complicated composition of MIEC cathodes. However, it would be difficult to develop design concept of key active interface of cathode for societal implementation of ‘state-of-the-art’ IT-SOFC device and system. To maximize the effect of MIEC particle addition and minimize the affection of negative factors such as Sr segregation effect for design of high quality cathode in IT-SOFC devices, the actual interface structure on the cathode [13] should be taken into account for development of new fabrication process such as decoration. Besides new fabrication process and modelling on the basis of model interface structure, the modelling based on microanalysis data should be used for the development of the active interface structure and useful production concept. As a consequence of this, the authors believe that the fusion of fabrication, characterization and modelling based on microanalysis data is the only way to develop the ‘state-of-the-art’ IT-SOFC device and system.

## 2. Electrolyte interface and electrolyte microstructure

The second key endeavor for the development of IT-SOFC is the control and stability of the microstructure in the solid electrolyte. In the previously published work, the formation of microdomain with the ordered structure of oxygen vacancies was clearly observed for  $\text{CaO}$  stabilized  $\text{ZrO}_2$  and  $\text{Sc}_2\text{O}_3$  stabilized  $\text{ZrO}_2$  electrolytes using analytical transmission electron microscopy (TEM) [5]. Since the defect interface change in the dense  $\text{ZrO}_2$  based solid electrolytes such as  $\text{CaO}$  stabilized  $\text{ZrO}_2$ ,  $\text{Sc}_2\text{O}_3$  stabilized  $\text{ZrO}_2$  and  $\text{Y}_2\text{O}_3$  stabilized  $\text{ZrO}_2$  is subtle in the microanalysis, the influence of microdomain formation on the electrolytic properties has been disregarded in the R & D field of high-temperature SOFC devices. However,  $\text{M}_2\text{O}_3$  doped  $\text{CeO}_2$  (M:  $\text{Gd}_2\text{O}_3$ ,  $\text{Y}_2\text{O}_3$ ,  $\text{Sm}_2\text{O}_3$ ,  $\text{La}_2\text{O}_3$  and so on) electrolytes which mainly consist of fluorite



structure, as well as  $\text{Y}_2\text{O}_3$  stabilized  $\text{ZrO}_2$  based solid electrolyte expose a unique feature of defect structure in TEM microanalysis. Especially, it was considered that  $\text{Gd}_2\text{O}_3$  doped  $\text{CeO}_2$  can be used as a solid electrolyte for IT-SOFC whose operation temperature is below  $500^\circ\text{C}$  in 2000 [14]. As a consequence of this, the microdomain structure in  $\text{M}_2\text{O}_3$  doped  $\text{CeO}_2$  (M:  $\text{Gd}_2\text{O}_3$ ,  $\text{Y}_2\text{O}_3$ ,  $\text{Sm}_2\text{O}_3$ ,  $\text{La}_2\text{O}_3$  and so on) dense sintered bodies were systematically observed using analytical TEM in the previously published works [15–24].

The key points of microdomain formation processes are summarized in figure 2. In general, easily sinterable powders are prepared by using a soft chemical processes such as sol-gel method, co-precipitation method and others. In this soft chemical process, the composition heterogeneity in nanoscale remains in the prepared nano-sized powders. During the sintering process to fabricate dense sintered bodies, nano-level dopant segregation, which is formed in the grain boundaries of electrolyte sintered bodies, seriously affects the size and distribution of the microdomains in the electrolytes [15–19]. While  $\text{Gd}_2\text{O}_3$  doped  $\text{CeO}_2$  electrolyte includes smaller microdomains and lower observed activation energy as compared with all of other  $\text{CeO}_2$  based solid electrolytes, the observed oxide ion diffusion becomes low level due to the formation of microdomains in the bulk. As a consequence of this, the microstructure design should be performed for stabilized  $\text{ZrO}_2$  electrolyte on the basis of microanalysis results obtained on  $\text{CeO}_2$  based electrolytes which mainly consist of fluorite structure.

### 3. Anode and anode/electrolyte interface

A third key endeavor for the development of IT-SOFCs is microstructure control in the anode layer. In previously published works, the ‘mixed ionic and electronic conducting (MIEC)’ particles such as Y-doped  $\text{SrTiO}_3$  was used in the cermet anode as well as LSM-based cathode [25]. In this case, both of nano-sized  $\text{CeO}_2$  and Ru (0.4 vol%) as co-catalyst were added into the anode with MIEC particles using the infiltration method, and chemical stability against  $\text{H}_2\text{S}$  in  $\text{H}_2$  fuel and performance of SOFC were improved. Also, it was reported that addition of  $\text{La}_{0.3}\text{Sr}_{0.7}\text{TiO}_3$  together with infiltration of  $\text{CeO}_2$  and Pd (0.5 wt%) [26], ceria doped with  $\text{Gd}_2\text{O}_3$  or  $\text{Sm}_2\text{O}_3$  infiltration, and  $\text{CeO}_x$ -Cu infiltration methods showed improvement of anode performance and chemical stability of anode to small amount of impurity  $\text{H}_2\text{S}$  in the fuel [27]. The previously reported infiltration technique using MIEC nano-particle and catalysts such as  $\text{CeO}_2$  and precious metal (less than 1 wt%) or Cu additives were useful for a lowering of excess overpotential on the anode and enhancement of the resistance to  $\text{H}_2\text{S}$  poisoning and carbon deposition (i.e. ‘coking’). However, it is not sufficient in order to minimize the precious metal or metal content and maximize the effect of improvement of anode performance. In addition, a distributed charge-transfer model analysis of Cu- and Ce- based IT-SOFCs well simulated the polarization and impedance spectra observed for Cu-Pd-mixture of  $\text{CeO}_2$  and  $\text{ZrO}_2/\text{Sm}$  doped  $\text{CeO}_2/\text{LSCF}$ -Gd doped  $\text{CeO}_2$  [28]. However, it would not be an easy task to develop design concept of active interface using experimental data simulation together with mass and charge conservation equations.

To design the active interface in the ‘state-of-the-art’ IT-SOFCs with the quality of exceeding the limit of conventional IT-SOFCs, the actual interfacial defect structure on the anode should be taken into account. Also, modelling on the basis of microanalysis data should be performed in order to propose the design paradigm for fabrication of ‘state-of-the-art’ IT-SOFC devices and systems. In the anode layer, the TPB areas are formed at the interface between Ni and electrolyte particle such as  $\text{CeO}_2$  doped with  $\text{Sm}_2\text{O}_3$ ,  $\text{Gd}_2\text{O}_3$  or  $\text{Y}_2\text{O}_3$  stabilized  $\text{ZrO}_2$ . STEM-EDS analysis examined the TPB area of an anode layer which consists of  $\text{M}_2\text{O}_3$  doped  $\text{CeO}_2$  (M:  $\text{Y}_2\text{O}_3$  or  $\text{Gd}_2\text{O}_3$ ) and Ni as shown in figure 3. In the narrow interface (i.e. width: approximately 200 nm) between doped  $\text{CeO}_2$  and Ni, C-type rare earth related superstructure formation was

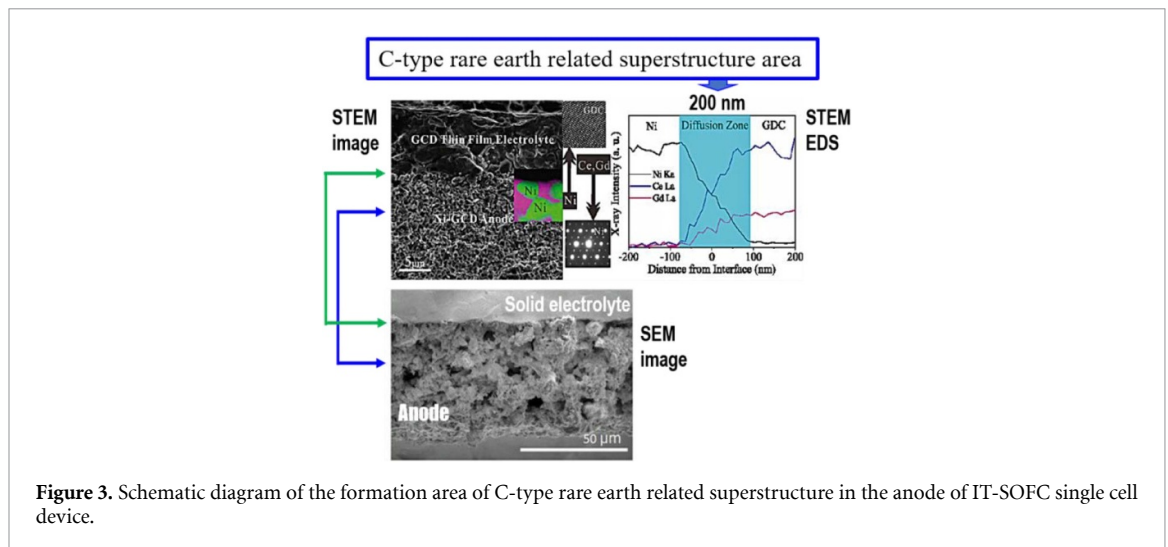


**Figure 3.** Schematic diagram of the formation area of C-type rare earth related superstructure in the anode of IT-SOFC single cell device.

clearly observed by STEM-EDS analysis [24, 29, 30]. To conclude the defect structure of C-type rare earth related superstructure well, the lattice statics modelling (Source code: GULP, empirical potential: Buckingham potential) was performed on the basis of analytical TEM microanalysis results (i.e. EELS analysis data and EDS analysis data) using workstation. This modelling indicates the small defect cluster which consists of dopant cation and oxygen vacancy is easily formed in the bulk of  $\text{CeO}_2$  based electrolyte [31] and at the interface of between Ni and  $\text{CeO}_2$  based electrolyte particle in the anode layer. This small defect cluster is easily combined with each other to form larger defect cluster in the narrow interface between Ni and  $\text{CeO}_2$  based particles. In addition, the oxygen vacancy position of large defect cluster agrees with that of C-type rare earth structure [24, 29–31]. It means that the lattice statics modelling on the basis of microanalysis data is quite useful to conclude the defect interface structural feature of SOFC device well.

In general, the simulation of fuel cell performance in ideal modelling field (i.e. the first-principles simulation) is performed for the design of high-quality IT-SOFC device. Recently, first-principles simulation in combination with already available data predicted an innovative breakthrough on the design of high-quality anode in IT-SOFCs [32]. This first-principles simulation work suggests that the surface oxide ion diffusion on YSZ in the cermet anode is the rate-determining step for the formation of water molecules in the fuel cell anode reaction below approximately 800 °C, although the dissociation rate constant of  $\text{H}_2$  on Ni is known to be high. In addition, this first principles simulation clearly indicates that the formation reaction of water molecules on the anode will be clearly enhanced, if we design the new active site for surface oxide ion diffusion on cubic  $\text{ZrO}_2$ . While the guide from the theoretical analysis is important, it is hard to create new active sites on the cubic  $\text{ZrO}_2$  surface using only data of first-principles simulations. This is because the real anode surface reaction is much more complicated as compared with the ideal anode reaction and additional factors which cannot be covered by theoretical analysis should be considered to design the new active sites on the real anode materials in IT-SOFCs.

To overcome this challenge, we tried to modify the defect structure at TPB on the Ni-cubic  $\text{ZrO}_2$  cermet anode by a combination of the lattice statics simulation and microanalysis of defect interface structure as well as combination analysis of Ni-cubic  $\text{CeO}_2$  cermet anode in the IT-SOFCs. As the authors mentioned in part 2 (electrolyte interface and electrolyte microstructure) and in the early part of the present part 3 (Anode and anode/electrolyte interface), the ordered structure of oxygen vacancy is formed as non-equilibrium defect at the interface of SOFC devices. This non-equilibrium defects is formed in the slow cooling process of fabrication of SOFC devices. In both  $\text{Y}_2\text{O}_3$  stabilized  $\text{ZrO}_2$  and  $\text{CeO}_2$  doped with  $\text{Sm}_2\text{O}_3$ ,  $\text{Gd}_2\text{O}_3$  or  $\text{Y}_2\text{O}_3$  systems, similar micro-domains with ordered structure of oxygen vacancy which can be assigned by C-type rare earth related structure were formed during fabrication process of SOFC devices. Also, its formation width at TPB area on the anode is quite narrow as we demonstrated in figure 3 such as 200 nm or less. In this narrow region, the amount of inactive lattice defect with C-type rare earth related defect structure would be in extremely low level such as 10 ppm ( $10 \text{ mg kg}^{-1}$ ) level. To modify this trace amount of inactive lattice defect for design of active site, the conventional infiltration process is not suitable. If the doping amount level is in too high level, different types clustering will occur in the defect interface region on the anode. Then, it is hard to expect the maximization of anode performance by using conventional infiltration method.

To activate the inactive defects at TPB on Ni-cubic  $\text{ZrO}_2$  cermet, we used trace amount of  $\text{PtO}_x$  whose content is approximately 10 to 100 ppm using sputtering technique [33]. The  $\text{PtO}_x$  was deposited on the



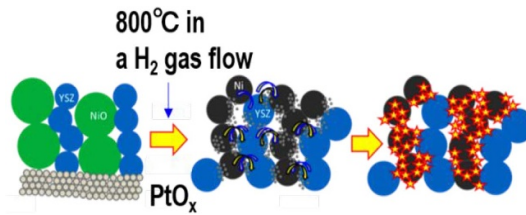


**Figure 4.** Schematic diagram of  $\text{PtO}_x$  sputtering process for activation of useless defects in superstructure at TPB on  $\text{Ni-Y}_2\text{O}_3$  stabilized cubic  $\text{ZrO}_2$  (YSZ) cermet anode in IT-SOFC.

**Table 1.** Assignment of extra reflections in selected area electron diffraction pattern recorded from the surface of Ni in the cermet anode with trace amount of Pt species and calculated binding energy on the basis of microanalysis data.

Lattice spacing of extra spots / nm	Assigned materials and lattice
0.152	PtO (200)
0.230	Pt (200)
0.164	unknown
0.199	Pt (311), NiO (222)
0.200	Pt (200), Pt (111)
0.204	Pt(200), Pt(111), Ni(111), NiO(200)

On partially oxidized Ni surface at near the three-phase boundary;

$$\Delta E_b \text{ of } V_{\text{Ni}}'' - \text{Pt}_i^{\bullet\bullet} - V_{\text{O}}^{\bullet\bullet} - \text{O}_i'' : 1.1 / \text{eV}$$

prepared  $\text{NiO}_x$ -8YSZ, conventional cermet anode, by means of magnetron sputtering as illustrated in figure 4.

The inductively coupled plasma mass spectrometry (ICP-MS) quantitatively analysed the Pt content in whole anode layer after reduction of anode layer at 800 °C in an  $\text{H}_2$  gas flow (i.e. the conventional conditioning process of the anode layer). After the conditioning process of the anode with trace amount of  $\text{PtO}_x$  (Pt content: approx. 10 to 100 ppm), we confirmed that the surface deposited Pt species were diffused into the anode layer by using analytical TEM, as we expected in figure 4.

The current density observed for the IT-SOFC single cell in which the  $\text{PtO}_x$  was deposited on the anode is approximately seven times higher than that of the IT-SOFC single cell without  $\text{PtO}_x$  at 700 °C, refer to figure 5 [33]. Also, the combination analysis of analytical TEM and lattice statics surface simulations (source code: GULP, empirical potential: Buckingham potential) confirmed that the defect interfacial structure located on partially oxidized Ni surface which is very close to TPB mainly consists of Pt cation (i.e.  $\text{Pt}^{2+}$  ( $\text{Pt}_i''$ )) and lattice vacancies such as oxygen vacancy ( $V_{\text{O}}''$ ) and interstitial oxygen ( $\text{O}_i''$ ), refer to table 1 [33].

The lattice statics surface simulation on the partially oxidized Ni surface along the guide of TEM microanalysis result shows high binding energy ( $\Delta E_b$ ) such as 1.1 eV. Note that high positive  $\Delta E_b$  value indicates the preferable cluster structure in the defect formation reaction. Also, the crystallographic defect cluster model indicates that buffer area for minimization of the lattice mismatch between cubic  $\text{ZrO}_2$  surface and partially oxidized Ni surface is formed at TPB area. And this buffer area would promote surface oxide ion diffusion (i.e. rate-determining step of anode reaction below 800 °C) from YSZ surface to Ni surface at TPB area. Then, it is concluded that the excess overpotential on the anode becomes low by modification of inactive non-equilibrium lattice defect at TPB area on the Ni surface. In contrast, the defect interfacial structure on cubic  $\text{ZrO}_2$  surface has not been identified due to the difficulty of observation of the defect structure with coherent interface for TEM sample. To overcome this difficulty for characterization of coherent interface defect structure, the first-principles surface simulation (source code: ABINIT, pseudopotential: PAW method) was performed using coherent interface model (i.e. Schottky defect model), refer to figure 6. This first-principles surface simulation provides us useful hint for design of active site on YSZ side. Our first-principles surface simulation suggests that di-valence (i.e.  $\text{Pt}^{2+}$ ,  $\text{Fe}^{2+}$ ) and tri-valence (i.e.  $\text{Rh}^{3+}$ ,  $\text{Fe}^{3+}$ ) cations create the useful defect cluster structure as active site at TPB area. In addition, our simulation suggests that defect cluster formation energy ( $\Delta E_f$ ) which is calculated by defect cluster with  $\text{Fe}^{3+}$  cation shows high negative value such as −5.8 eV. Note that high negative  $\Delta E_f$  value indicates the preferable cluster structure in the defect formation reaction.

In addition, XPS analysis clearly detected  $\text{Fe}^{3+}$  species from the interface of Ni and cubic  $\text{ZrO}_2$  after conventional conditioning process (i.e. reduction of anode at 800 °C in  $\text{H}_2$  gas flow) (unpublished work).

This combination work of surface microanalysis and predictive first-principles surface simulation indicates that active site is created by  $\text{Fe}^{3+}$  species doping on cubic  $\text{ZrO}_2$  at TPB. Namely, the anode performance can be improved using  $\text{Fe}^{3+}$  species instead of  $\text{Pt}^{2+}$  species. Along the guide of this

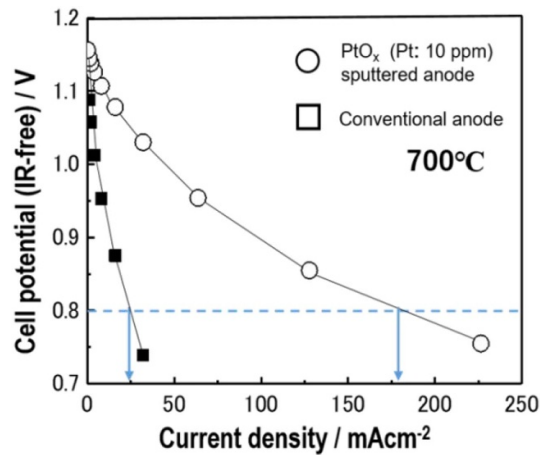


**Figure 5.** Current density vs. cell potential (IR-free) observed for trace amount of PtO<sub>x</sub> (Pt content: 10 ppm) sputtered anode and conventional anode. Anode: YSZ-Ni cermet anode (YSZ/Ni = 1/4), anode gas: humidified H<sub>2</sub> gas (80 ml min<sup>-1</sup>), cathode: commercially available LSM (LSM20-I, Fuel Cell Materials. Com, USA), cathode gas: O<sub>2</sub> gas (80 ml min<sup>-1</sup>), operation temperature: 700 °C.

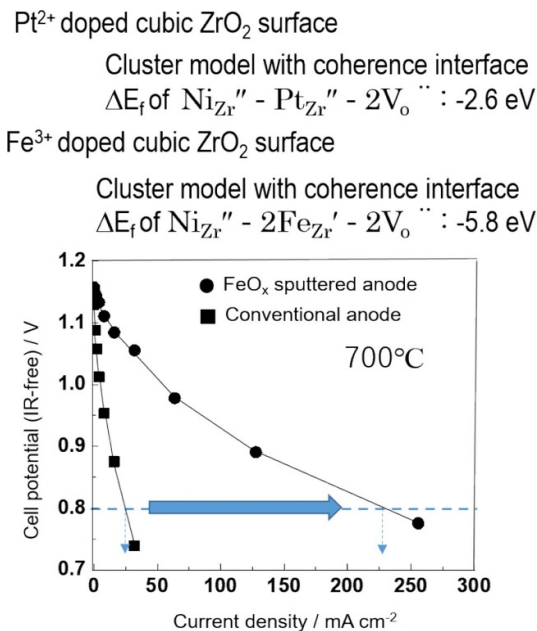


**Figure 6.** Defect formation energies (ΔE<sub>f</sub>) calculated by coherent interface model and cell potential as a function of current density observed for small amount of FeO<sub>x</sub> sputtered anode and conventional anode. Operation condition is same as figure 5.

combination work, our multidisciplinary team successfully observed the improved anode performance using small amount of FeO<sub>x</sub> sputtered sample (i.e. Fe content: approximately 1000 ppm) as well as PtO<sub>x</sub> sputtered sample, refer to figure 6) [34].

#### 4. Summary

The data which are described in sections 1 to 3 clearly suggest the importance of multidisciplinary research work as shown in figure 7. To see new breakthroughs for the design of 'state-of-the-art' next generation IT-SOFC devices, we must carefully characterize key defect interface structure in our devices. Also, we must perform the lattice statics surface and bulk simulation to conclude the key interface defect structure at TPB area. Then we must modify the interfaces on the basis of suggestion of combination analysis of microanalysis and surface modelling. If our model is reasonable, we will see improved properties from our IT-SOFC devices. After we confirm such the improvement of IT-SOFC device performance, more careful microanalysis such as operando-microanalysis and high precision modelling (i.e. first-principles simulation) for the design of high-quality TPB in the interfaces of IT-SOFCs are required. Through such an interactive

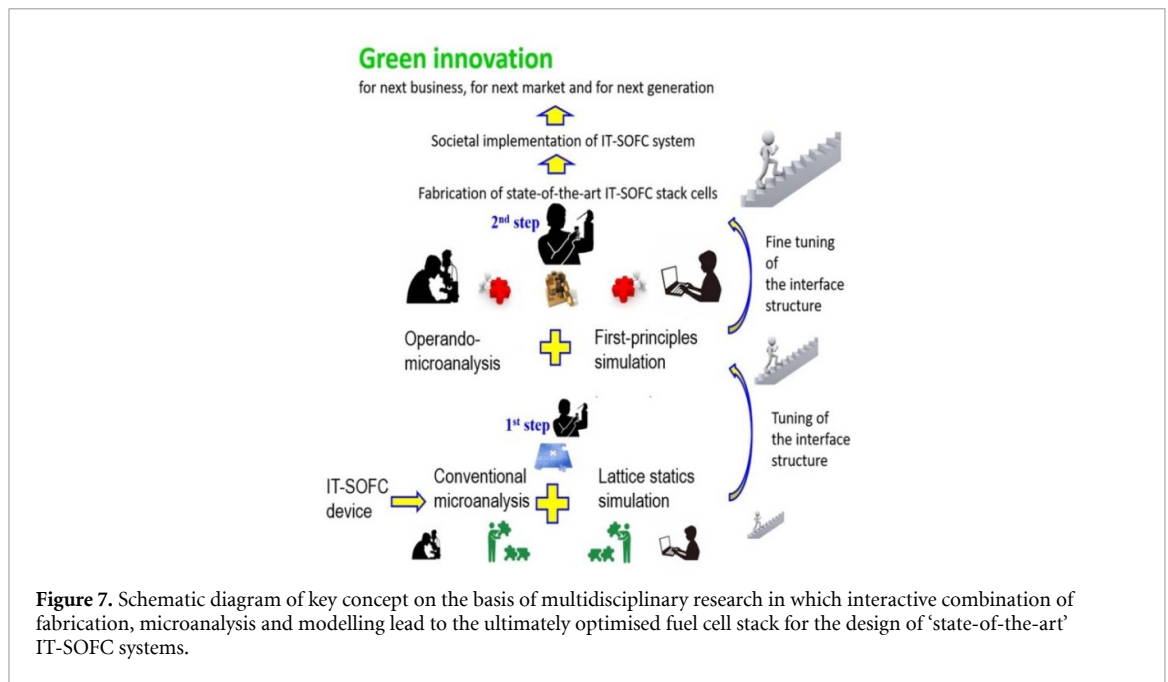


**Figure 7.** Schematic diagram of key concept on the basis of multidisciplinary research in which interactive combination of fabrication, microanalysis and modelling lead to the ultimately optimised fuel cell stack for the design of 'state-of-the-art' IT-SOFC systems.

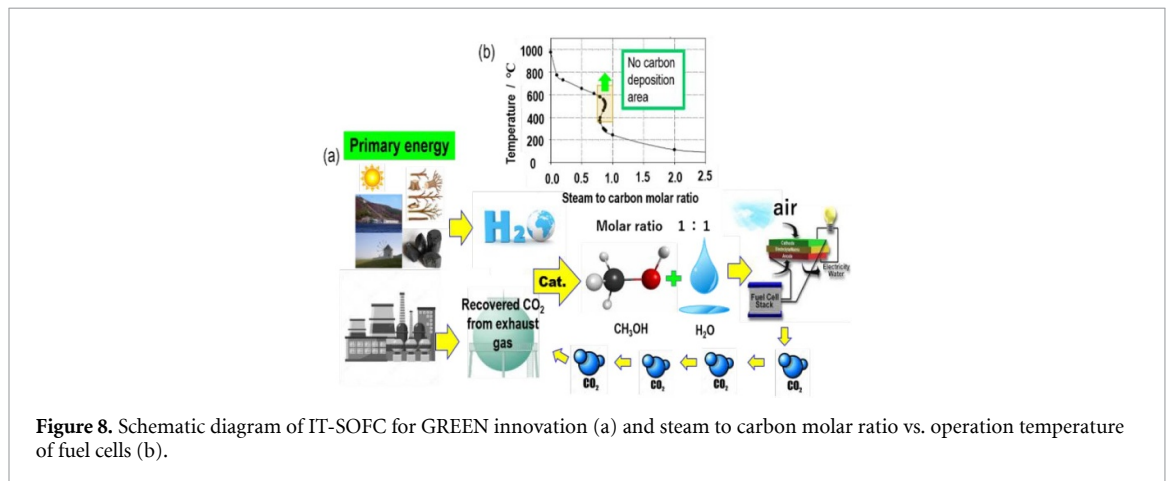


**Figure 8.** Schematic diagram of IT-SOFC for GREEN innovation (a) and steam to carbon molar ratio vs. operation temperature of fuel cells (b).

design concept by fusing fabrication, micro-characterization and modelling knowledge, we have a much greater opportunity to purpose (target) design new electrode materials for GREEN innovations.

In general, the GREEN innovation is defined as technical innovations that consist of new or modified processes, practices, systems and products which benefit the environment and so contribute to environmental sustainability [35]. To establish the sustainable society through the formation of hydrogen society, R & D challenges for high quality polymer electrolyte membrane fuel cell (PEMFC) device and system or high power all solid state Li ion battery is very popular in the world. Certainly, hydrogen which is created by primary energy can be directly used for PEMFC system. In this case, however, there may be little chances to use the stored greenhouse gas (i.e.  $CO_2$  gas) which is recovered from exhausted gas well.

As illustrated in figure 8(a),  $H_2$  and  $CO_2$  gas can be converted to mixture of  $H_2O$  and  $CH_3OH$  ( $H_2O/CH_3OH$  molar ratio = 1) on the conventional catalyst. Then, this mixture gas can be used as fuel for SOFC device and system for generation of electricity in high efficiency. In this case, PEMFC can be used as backup generator to cover the peak electricity demand in summer season and in day time of industrial work. In this case, the deposition of carbon (i.e. 'coking') would be one of problems for design of 'state-of-the-art' IT-SOFC device with good balance of high performance and good durability. It is well-known that the 'coking' is depressed along the guide of previously reported the relationship between steam/carbon molar ratio in the fuel and operation temperature of SOFCs, refer to figure 8(b) [36].

When we use the mixture of  $H_2O$  and  $CH_3OH$  ( $H_2O/CH_3OH$  molar ratio = 1) as fuel for IT-SOFC device, this fuel composition would be in boundary region between risky region of 'coking' (below the line in figure 8(b)) and the safety region (over the line in figure 8(b)). This point can be shifted to the safety region side in IT-SOFC operation by improvement of kinetics at TPB on the anode. Then, we will have great



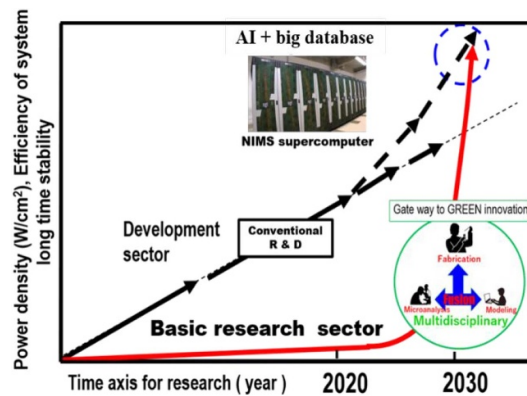


**Figure 9.** Schematic diagram of future prospects of research and development work for 'state-of-the-art' IT-SOFC device and system by fusion of fabrication, microanalysis and modelling.

opportunity to see GREEN innovation by development of high-quality system with 'state-of-the-art' IT-SOFC in the near future.

Of course, we must make good balance between resources, production cost, high quality performance and long operation durability for economical, ecological and environmental implementation of the 'state-of-the-art' next generation IT-SOFC devices during such an endeavour. It is well-known that e.g. the performance of IT-SOFC devices were degraded by many factors such as carbon deposition on the anode [37], chromium deposition/poisoning on the cathode [38] and micro-domain growth in solid electrolyte [5, 14] in the IT-SOFCs. Those important information are now available in big database. We know that the combination of artificial intelligence (AI) and big database will accelerate the conventional style of R&D innovative work (i.e. incremental technical innovation). However, there is serious weakness in this combination approach. It is 'null set' of big database. Our suggested multidisciplinary research work will input new data (i.e. something new) in the 'null set' of big database and overcome the weakness of AI/big database combination work for the design of the 'state-of-the-art' next generation IT-SOFCs.

With the uptake of this approach and the availability of AI, the authors predict a GREEN innovation wave in the solid oxide full cells development to happen up to 2030 by a combination of AI/big database and our suggested multidisciplinary reference based work in R & D, refer to figure 9.

As explained in this prospect, the conventional modelling on the basis of kinetics and thermodynamics without microanalysis data can simulate polarization experiments and impedance experiments well. It would be useful for optimization of complicated composition of composite cathode and anode. However, it would be scientifically insufficient to complete the societal implementation of the 'state-of-the-art' IT-SOFC device and system, referring to the part 1 (cathode and cathode/electrolyte interface) and part 3 (anode and anode/electrolyte interface).

After we input the data of interactive works between fabrication and modelling on the basis of microanalysis results of the defect interface into the big database, the deep learning by combination of AI and the big database which includes both data of conventional modelling and our proposed modelling based on the real defect interface will evolve the fabrication techniques and modelling techniques for the social implementation of 'state-of-the-art' IT-SOFC device and system within one decade. That is one typical example of radical innovation as schematically suggested in figure 9.

We foresee that the proposed optimised material development concept will be helpful for acceleration of R&D of the next generation of IT-SOFCs and open the door for a next GREEN innovation wave in the fuel cell field.

## Acknowledgments

The authors express our sincere gratitude to the members of our international collaboration team (i.e. PhD students, postdoctoral researchers, and research assistant staffs in each research team) for the development of the international collaboration between Japan and Australia.

## Funding

This work was partially supported by JSPS Joint Research Project (Open Partnership) under bilateral program between Japan and Australia (FY 2019- FY2020, DG 1270) and Australian Research Council (DP180100731). Also, the present work was additionally supported by the Global Research Center for Environmental and Energy based on the Nanomaterials Science (GREEN), National Institute for Materials Science (NIMS), Japan.

## ORCID iDs

Toshiyuki Mori  <https://orcid.org/0000-0003-3199-2498>

San Ping Jiang  <https://orcid.org/0000-0002-7042-2976>

## References

- [1] Goodenough J B and Huang Y H 2007 *J. Power Sources* **173** 1–10
- [2] Jacobson A J 2010 *Chem. Mater.* **22** 660–74
- [3] Wang S Y and Jiang S P 2017 *Natl. Sci. Rev.* **4** 163–6
- [4] Chen K, Li N, Ai N, Li M, Cheng Y, Rickard W D A, Li J and Jiang S P 2016 *J. Mater. Chem. A* **4** 17678–85
- [5] Drennan J 1998 *J. Mater. Syntn. Process.* **6** 181–9
- [6] Jiang S P 2008 *J. Mater. Sci.* **43** 6799–833
- [7] Jiang S P 2012 *Int. J. Hydrogen Energy* **37** 449–70
- [8] Jiang S P 2019 *Int. J. Hydrogen Energy* **44** 7448–93
- [9] Steele B C H 2000 *Solid State Ion.* **129** 95–110
- [10] He S, Zhang Q, Maurizio G, Catellani L, Chen K, Chang Q, Santarelli M and Jiang S P 2018 *ACS Appl. Mater. Interfaces* **10** 40549–59
- [11] Donazzi A, Cordaro G, Baricci A, Ding Z-B and Maestri M 2020 *Electrochem. Acta* **335** 135620
- [12] Laurencin J, Hubert M, Couturier K, Bihan T L, Cloetens P, Lefebvre-Joud F and Siebert E 2015 *Electrochem. Acta* **335** 1299–316
- [13] He S, Saunders M, Chen K, Gao H, Suvorova A, Rickard W D A, Quadir Z, Cui C Q and Jiang S P 2018 *J. Electrochem. Soc.* **165** F417–29
- [14] Mori T, Drennan J, Lee J-H, Li J G and Ikegami T 2002 *Solid State Ion.* **154** 461–6
- [15] Mori T, Drennan J, Wang Y, Auchterlonie G, Li J G and Yago A 2003 *Sci. Technol. Adv. Mater.* **4** 213–20
- [16] Mori T, Wang Y, Drennan J, Auchterlonie G, Li J G and Ikegami T 2004 *Solid State Ion.* **175** 641–9
- [17] Ou D R, Mori T, Ye F, Takahashi M, Zou J and Drennan J 2006 *Acta Mater.* **54** 3737–46
- [18] Mori T and Drennan J 2006 *J. Electroceram.* **17** 749–57
- [19] Ou D R, Mori T, Ye F, Kobayashi T, Zou J, Auchterlonie G and Drennan J 2006 *Appl. Phys. Lett.* **89** 171911
- [20] Ou D R, Mori T, Ye F, Zou J and Drennan J 2007 *Electrochem. Solid State Lett.* **10** 1–3
- [21] Ou D R, Mori T, Ye F, Zou J and Drennan J 2008 *Phys. Rev. B* **77** 024108
- [22] Li Z P, Mori T, Auchterlonie G, Zou J and Drennan J 2011 *Appl. Phys. Lett.* **98** 093104
- [23] Li Z P, Mori T, Auchterlonie G, Zou J and Drennan J 2012 *Mater. Res. Bull.* **47** 763–7
- [24] Li Z P, Mori T, Auchterlonie G, Guo Y, Zou J, Drennan J and Miyayama M 2011 *J. Phys. Chem. C* **115** 6877–85
- [25] Kurokawa H, Yang L, Jacobson C P, De Jonghe L C and Visco S J 2007 *J. Power Sources* **164** 510–8
- [26] Lee S, Kim G, Vohs J M and Gorte R J 2008 *J. Electrochem. Soc.* **155** B1179–83
- [27] Liu Z, Liu B, Ding D, Liu M, Chen F and Xia C 2013 *J. Power Sources* **237** 243–59
- [28] Rahmanipour M, Pappacena A, Boaro M and Donazzi A 2017 *J. Electrochem. Soc.* **164** F1249 – 64
- [29] Li Z P, Mori T, Ye F, Ou D R, Zou J and Drennan J 2011 *Phys. Rev. B* **84** 180201(R)
- [30] Li Z P, Mori T, Zou J and Drennan J 2012 *Phys. Chem. Chem. Phys.* **14** 8369–75
- [31] Ye F, Mori T, Ou D R and Cormack A N 2009 *Solid State Ion.* **180** 1127–32
- [32] Liu S, Muhammad A, Mihara K, Ishimori T, Tada T and Koyama M 2017 *J. Phys. Chem. C* **121** 19069–79
- [33] Rednyk A, Mori T, Yamamoto S, Suzuki A, Yamamoto Y, Tanji T, Isaka N, Kus P, Ito S and Ye F 2018 *ChemPlusChem* **83** 756–68
- [34] Tong K, Mori T and Ye F 2019 Role of doped  $\text{Pt}^{2+}$  or  $\text{Rh}^{3+}$  for promotion of the oxygen vacancy formation and diffusion on  $\text{ZrO}_2$  (111) surface: a first-principles study *Extended abstract of The 13th Pacific Rim Conf. of Ceramic Societies (PACRIM13)* (27 October–1 November, 2019) vol 28-C1 (Japan: Okinawa Convention Center) p S15-15 [www.researchgate.net/publication/338779266\\_PACRIM\\_13\\_Dr\\_Ke\\_Tong](http://www.researchgate.net/publication/338779266_PACRIM_13_Dr_Ke_Tong)
- [35] Introduction of Green innovation definition in homepage of Cambridge innovation and intellectual property management laboratory (Cambridge: Cambridge University Press)
- [36] Energy and Environmental Solutions 2000 *Fuel Cell Handbook, Fifth Edition* (United States: U.S. Department of Energy) <https://doi.org/10.2172/769283>
- [37] Yue W et al 2019 *Nano Energy* **62** 64–78
- [38] Jiang S P and Chen X 2014 *Int. J. Hydrogen Energy* **39** 505–31